Myogenic Akt signaling upregulates the utrophin–glycoprotein complex and promotes sarcolemma stability in muscular dystrophy

Angela K. Peter[1],[†], Christopher Y. Ko[1],[†], Michelle H. Kim[1], Nigel Hsu[1], Noriyuki Ouchi[3], Suhn Rhie[1], Yasuhiro Izumiya[3], Ling Zeng[3], Kenneth Walsh[3] and Rachelle H. Crosbie[1],[2],*

[1]Department of Physiological Science and [2]Molecular Biology Institute, University of California, Los Angeles, CA 90095, USA and [3]Molecular Cardiology, Whitaker Cardiovascular Institute, Boston University School of Medicine, Boston, MA 02118, USA

Duchenne muscular dystrophy is caused by dystrophin mutations that lead to structural instability of the sarcolemma membrane, myofiber degeneration/regeneration and progressive muscle wasting. Here we show that myogenic Akt signaling in mouse models of dystrophy promotes increased expression of utrophin, which replaces the function of dystrophin thereby preventing sarcolemma damage and muscle wasting. In contrast to previous suggestions that increased Akt in dystrophy was a secondary consequence of pathology, our findings demonstrate a pivotal role for this signaling pathway such that modulation of Akt can significantly affect disease outcome by amplification of existing, physiological compensatory mechanisms.

INTRODUCTION

Muscular dystrophy describes a group of genetic disorders generally characterized by progressive muscle weakness. The most common form of muscular dystrophy, Duchenne muscular dystrophy (DMD), is caused by primary mutations in the dystrophin gene (1–3). DMD is characterized by progressive muscle weakness eventually leading to cardiac and respiratory failure. Dystrophin deficiency alters the stability of the entire dystrophin-glycoprotein complex (DGC) resulting in reduction of the entire complex at the plasma membrane (for review 4). In skeletal muscle fibers, the core components of the DGC include dystrophin, the dystroglycans (α- and β-DG), the sarcoglycans (α-, β-, γ- and δ-SG), sarcospan (SSPN) and the syntrophins (for review 5). Peripheral and integral membrane components of the DGC provide a physical connection between the extracellular matrix and the intracellular actin cytoskeleton (3,6–10). Loss of dystrophin and the DGC alters the integrity of the sarcolemma, the skeletal muscle plasma membrane, increasing contraction-induced

damage. Even though skeletal muscle possesses the innate ability to regenerate, this ability is insufficient to compensate for the structural damage endured during muscle contraction in DMD patients. Thus, the link between the extracellular membrane and the intracellular cytoskeleton provided by the DGC is essential for maintaining sarcolemmal stability.

The regenerative capacity of skeletal muscle is insufficient in combating persistent and widespread degeneration of myofibers with structural defects in the sarcolemma. Akt, a serine/threonine protein kinase, has previously been shown to be altered in both DMD patients and in dystrophin-deficient *mdx* mice (11,12). Previous reports indicate that activation of the phosphatidylinositol 3-kinase (PI(3)K)/Akt pathway is critical for the activation of muscle hypertrophy (13–17). We and others have established that the same PI(3)K/Akt signaling pathways responsible for inducing skeletal muscle hypertrophy (13) are also activated in many forms of muscular dystrophy (11,12). Furthermore, we have recently demonstrated that direct manipulation of Akt in normal, wild-type (WT) mice induces skeletal muscle hypertrophy that results

---

*To whom correspondence should be addressed at: Department of Physiological Science, University of California Los Angeles, 621 Charles E. Young Drive South, Life Sciences Building Room 5804, Los Angeles, CA 90025, USA. Tel: +1 3107942103; Fax: +1 3102063987; Email: rcrosbie@physci.ucla.edu
†These authors contributed equally to this work.

in dramatic improvements in force generation while decreasing adipose mass (18). Taken together, these previous reports indicate activation of Akt in dystrophic muscle may be a key mediator of the hypertrophic response both in the promotion of muscle hypertrophy and in blood vessel recruitment.

The Akt family of protein kinases is activated by numerous extracellular stimuli transduced across the membrane through membrane-bound receptor tyrosine kinases (for review 20). Akt is then recruited to the plasma membrane through activation of PI(3)K. Subsequent phosphorylation releases Akt from the plasma membrane and leads to translocation of phosphorylated Akt (P-Akt) to the cytoplasm and activation of downstream targets. Although recent research has reported Akt translocation to the nucleus following activation (for review 20), Akt remains in the cytosolic fraction following activation in skeletal muscle (11). We have created a skeletal muscle-specific, conditional transgenic mouse expressing a constitutively active form of Akt (18). In this study, an increase in Akt activation in skeletal muscle led to muscle hypertrophy specifically in type IIb fibers. The induction of hypertrophy was also accompanied by increased fiber strength, decreased fat mass and improvement of metabolic parameters (18). These findings indicate that Akt activation alone can increase muscle mass and improve muscle strength.

In the current report, we examined the effect of constitutive Akt activation on the dystrophic pathology in dystrophin-deficient *mdx* mice. We demonstrate that activation of the Akt transgene at the prenectroic (<3.5 weeks of age) stage of disease delays the onset of dystrophic pathology in *mdx* mice. We exploited the conditional transgene (18) to activate the transgene for a total of 3 weeks before analyzing the tissue for signs of muscular dystrophy. We show an increase in muscle hypertrophy and decreased sarcolemmal fragility in Akt-treated *mdx* mice compared with the untreated *mdx* controls. The mechanism of amelioration involves increased expression and wider distribution of adhesion complexes including the utrophin–glycoprotein complex (UGC). Overexpression of the UGC has previously been shown to ameliorate the dystrophic pathology in *mdx* mice (21,22). These findings suggest that the overexpression and extra-synaptic localization of the UGC and integrin compensate for the loss of the DGC in Akt-transgenic, *mdx* mice. This current study identifies myogenic Akt signaling as a drug target that could improve the muscle wasting and sarcolemmal fragility associated with muscular dystrophy by increasing expression of the UGC.

RESULTS AND DISCUSSION

Generation of *mdx* mice with inducible Akt1 expression in skeletal muscle

To investigate whether the beneficial effects of Akt would manifest in dystrophic muscle, we engineered mice with muscular dystrophy to express Akt1 by introducing the *TRE-myrAkt1* and *MCK-rtTA* transgenes (18) into dystrophin-deficient *mdx* mice (Fig. 1). Offspring that had inherited only one of the *TRE-myrAkt1* or *MCK-rtTA* transgenes are referred to as single-transgenic (STG) mice and lack the means for the conditional activation of Akt1. Double-transgenic (DTG) offspring inherited both of the transgenes and increase expression of Akt1 upon dox-
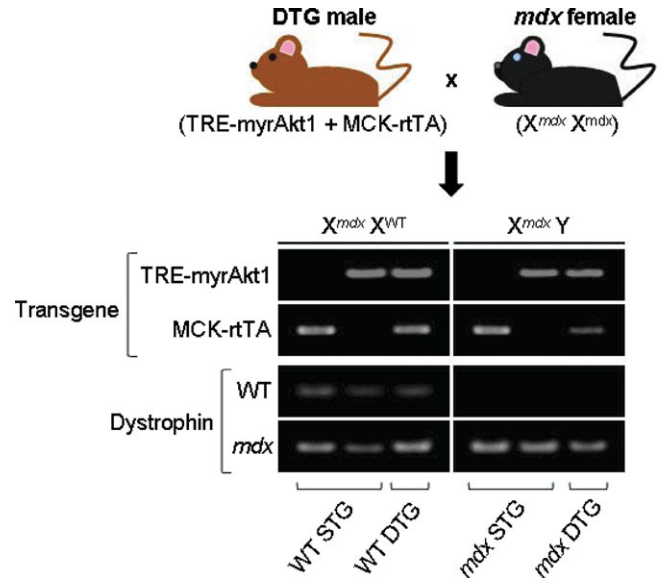

Figure 1. Generation of Akt-transgenic *mdx* mice. Breeding scheme and genotyping of offspring by PCR amplification. Double-transgenic (*TRE-myrAkt1 + MCK-rtTA*) male mice on a wild-type (WT) dystrophin background were crossed with *mdx* females. Each transgenic offspring inherited either one or both of the Akt transgenes (*TRE-myrAkt1, MCK-rtTA*). All female offspring, which were heterozygous for dystrophin ($X^{mdx} X^{WT}$) and expressing non-dystrophic phenotypes, are denoted as being either wild-type single-transgenic (WT STG) or wild-type double-transgenic (WT DTG). All male offspring possessed *mdx* genotypes ($X^{mdx} Y$) and are denoted as being either *mdx* STG or *mdx* DTG. Transgenic offspring were genotyped through two pairs of PCR amplification reactions. In the first pair of reactions, offspring were genotyped for the two transgenes responsible for the activation of constitutively active Akt1. In the first PCR reaction, the transgene for the constitutively active form of Akt1 under the control of a tetracycline responsive promoter (*TRE-myrAkt1*) is amplified, yielding a 380 bp product. In the second PCR reaction, the transgene expressing a reverse tetracycline transactivator under the control of a modified muscle creatine kinase promoter (*MCK-rtTA*) was amplified, yielding a 567 bp product. In the second pair of reactions, offspring were genotyped for the *mdx* locus. The forward primers used in this pair of reactions are identical. In the first reaction of the pair, the WT allele was amplified using a WT allele-specific reverse primer. In the second reaction, the *mdx* allele was amplified using an *mdx* allele-specific reverse primer. Each reaction in this pair yielded a 275 bp product.

ycycline (DOX) treatment. All female offspring are heterozygous for dystrophin ($X^{mdx}X^{WT}$) and display a non-dystrophic phenotype, so they are referred to as WT mice. Male offspring, described here as *mdx* mice, inherited only the deficient copy of dystrophin on the X chromosome ($X^{mdx}Y$) and display a dystrophic phenotype without Akt activation. PCR analysis was used to confirm the six possible genotypes of transgenic offspring which are categorized into the following four groups: WT STG, WT DTG, *mdx* STG and *mdx* DTG.

DOX-induced Akt overexpression causes muscle hypertrophy in mdx mice

Similar to DMD patients, *mdx* mice possess a genetic mutation in the dystrophin gene, resulting in loss of dystrophin protein and the entire DGC (1–6). The peak necrotic stage of disease occurs in *mdx* mice when they are between 3 and 6 weeks of age and when the frequency of degeneration/regeneration is at its greatest (23). In our model system, DOX, required for transgene activation, was administered at the prenecrotic
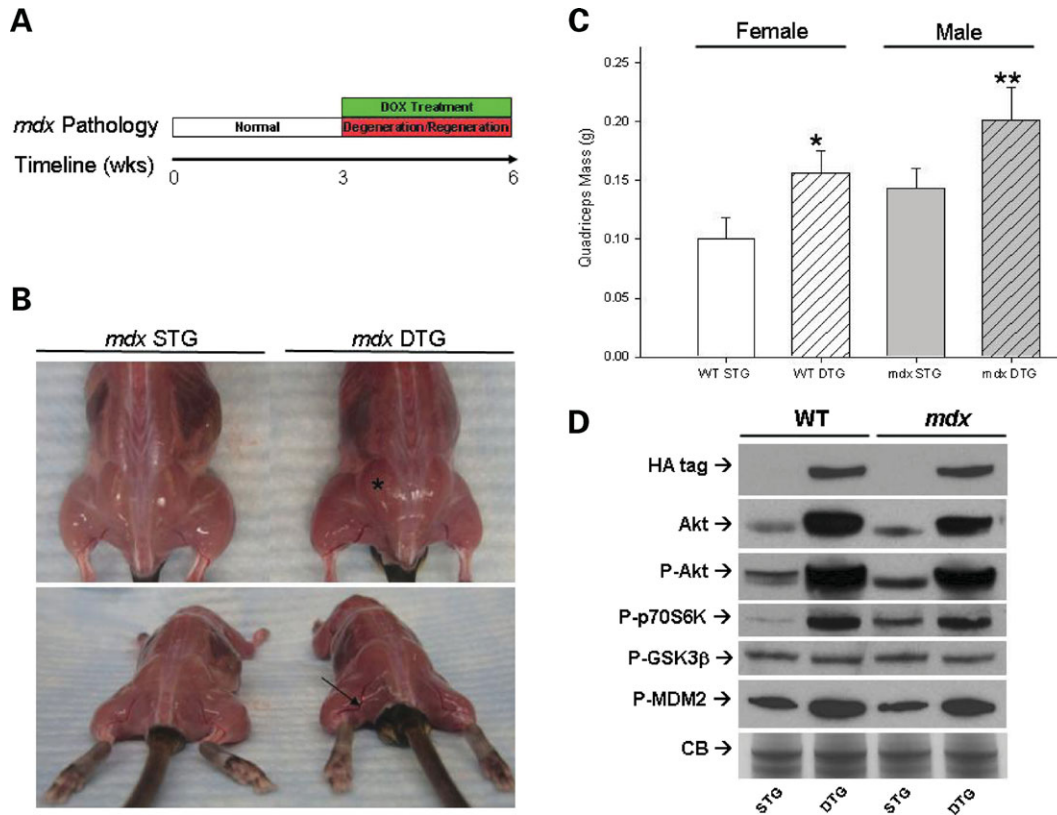
Figure 2. Akt1 activation increases muscle mass in *mdx* mice. (**A**) Timeline of doxycycline (DOX) treatment of Akt STG and DTG mice. At three weeks of age, the mice were treated with DOX, inducing Akt expression in Akt DTG mice for a total of three weeks. DOX treatment period corresponds to period of maximal myofiber degeneration and regeneration in *mdx* mice. Tissues were analyzed at six weeks of age. (**B**) Representative images of *mdx* STG and *mdx* DTG mice reveal dramatic differences in muscle mass. DTG mice display increased muscle mass (asterisk) and hypervascularization (arrow) after three weeks of transgene activation. (**C**) Activation of Akt significantly increases muscle mass in DTG mice. Induction of transgene in DTG mice significantly increases total quadriceps weight when compared to their WT (Fisher's, $*P < 0.00001$) and *mdx* STG (Fisher's, $**P < 0.005$) counterparts. Quadriceps weights are represented as an average of the left and right quadriceps of each animal. Bars represent mean quadriceps weights ($\pm$ SEM; $n = 21$ *mdx* STG, $n = 4$ *mdx* DTG. $n = 18$ WT STG, $n = 11$ WT DTG). (**D**) Immunoblotting for Akt pathway proteins. Akt pathway proteins were detected from total skeletal muscle lysates of six-week-old WT STG, WT DTG, *mdx* STG, and *mdx* DTG mice. Identical membranes were probed with antibodies against Akt, P-Akt, P-70S6K, P-GSK3β, P-MDM2, and the HA-tag engineered onto the Akt1 transgene, as indicated. Coomassie blue staining of total protein is shown on the bottom panel (CB Stain) as a loading control. Activation of Akt for three weeks is sufficient for activation of P-70S6K in the Akt signaling axis. Furthermore, P-MDM2 levels increase upon Akt activation whereas P-GSK3β levels remain constant.

stage of disease and mice were analyzed during peak necrosis (Fig. 2A). Increased Akt1 signaling induced obvious hind limb hypertrophy and hypervascularization in *mdx* mice (Fig. 2B) and increased quadriceps mass by 60% in WT (Fisher's $P < 0.00001$) and by 35% in *mdx* DTG mice (Fisher's $P < 0.005$) relative to their respective STG controls (Fig. 2C). Muscles from both male and female mice displayed similar levels of increased muscle mass upon transgene activation (Supplementary Material, Fig. S1). Immunoblotting skeletal muscle protein lysates revealed comparable expression and functionality of the Akt transgene in treated WT and *mdx* DTG mice. Detection of exogenous Akt was facilitated by a hemagglutinin (HA) tag engineered onto the *TRE-myrAkt1* transgene. Induction of Akt transgene was restricted to DTG muscle, while STG controls with either the *TRE-myrAkt1* or *MCK-rtTA* transgenes lacked conditional Akt activation (Fig. 2D). The level of total Akt protein overexpression in DTG muscle was increased by 2-fold relative to STG controls (Supplementary Material, Fig. S2). DTG muscle also exhibited activation of p70[S6K] and MDM2 (Fig. 2D). p70[S6K] is a downstream effector molecule

in the mammalian target of rapamycin (mTOR) pathway which amplifies protein translation and MDM2 functions in part to enhance MyoD-controlled differentiation and transcription (24).

We found that Akt activation increased cross-sectional myofiber area in quadriceps muscle from both WT and *mdx* DTG mice (Fig. 3A and B). The distribution of fiber cross-sectional areas (CSAs) reveals increases in larger fibers ($4500–7500 \ \mu m^2$) for DTG mice (Fig. 3B). Central nucleation, a marker for fiber regeneration, was elevated in *mdx* muscle (ANOVA, $P < 0.005$) and Akt activation in *mdx* mice did not significantly alter the frequency of central nucleation in *mdx* mice (Fig. 3C).

Improved sarcolemmal integrity upon Akt1 expression in *mdx* DTG mice

Loss of dystrophin and the DGC in *mdx* mice and in DMD patients results in contraction-induced sarcolemmal disruption and instability. Sarcolemmal integrity in *mdx* DTG mice was
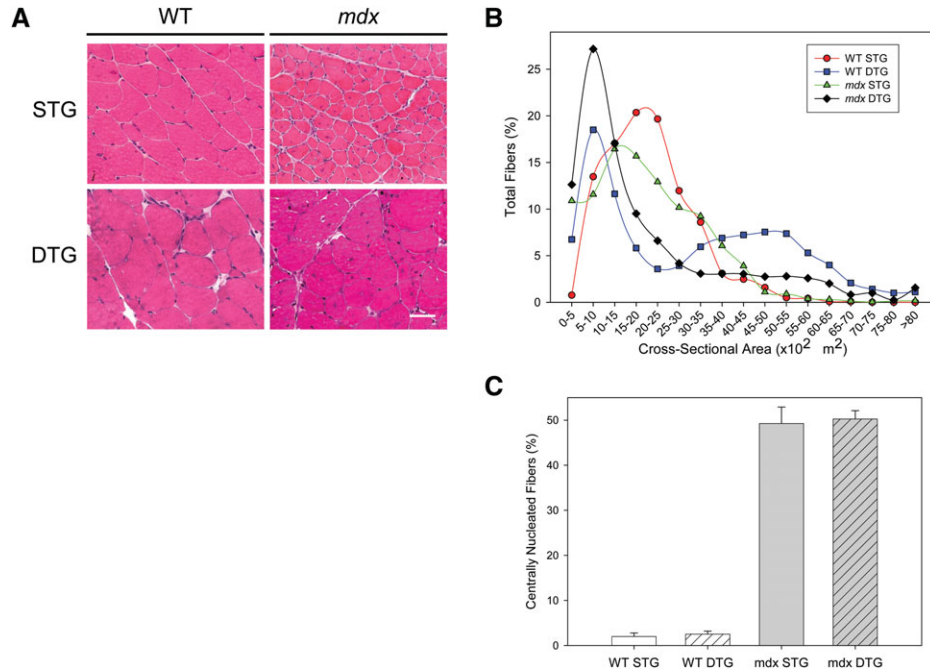
Figure 3. Akt1 activation increases fiber hypertrophy. (**A**) Transverse quadriceps muscle sections from six-week-old WT STG, WT DTG, *mdx* STG, and *mdx* DTG mice were stained with hematoxylin and eosin (H&E) to visualize muscle histology. Constitutive Akt activation in *mdx* DTG mice did not reduce the prevalence of centrally nucleated fibers and necrosis when compared to non-phenotypic littermates. Note the muscle fiber hypertrophy in both groups of DTG mice. Bar, 50 μm. (**B**) Distribution of cross sectional fiber areas of quadriceps muscle. DTG mice exhibit greater populations of both smaller and hypertrophic fibers compared to their WT and *mdx* STG controls. (**C**) Central nucleation (% of total fibers) in quadriceps muscle sections was quantified in each group of mice. *Mdx* mice exhibit significantly higher levels of central nucleation when compared to WT mice (*ANOVA, $P < 0.005$). However, DTG mice do not exhibit significant differences in the amount of central nucleation when compared to their STG control littermates. Central nucleation is represented as an average of the % of central nucleation of the left and right quadriceps of each animal. Bars represent mean central nucleation. ($n = 3$ WT STG, $n = 2$ WT DTG, $n = 2$ *mdx* STG, $n = 3$ *mdx* DTG.).

examined by the Evan's Blue Dye (EBD) tracer assay, which allows assessment of blood serum albumin infiltration into damaged muscle fibers. The quadriceps muscles of *mdx* STG mice displayed elevated levels of EBD infiltration compared with WT STG and DTG controls (Fig. 4A) due to the sarcolemmal fragility in *mdx* muscle. In contrast, Akt induction ameliorated sarcolemmal damage in *mdx* DTG mice to nearly WT DTG control levels (Fig. 4B; Student's t-test with Bonferroni adjustment, $P < 0.03$).

Akt activates muscle regeneration

The observation that central nucleation was unaffected in *mdx* DTG mice suggested that myofibers were undergoing regeneration despite restoration of membrane stability. Based on previous observations that Akt is involved in proliferation of satellite cells (25), we postulated that regeneration in *mdx* DTG muscle resulted from activation of satellite cells in Akt over-expressing muscle. In order to test this observation, we determined the myofiber CSA for WT DTG muscle after 2, 4 and 6 weeks of Akt1 transgene activation. For these studies, we chose to induce Akt activation in adult WT mice to avoid any complications of disease pathology that occur in mdx muscles (i.e. diaphragm, soleus, cardiac and EDL muscles do not express the Akt1 transgene) in this model (18). Myofiber CSA doubled after 2 weeks of Akt1 activation (Fig. 5A and B). An additional 2 weeks of *Akt1* transgene acti-

vation increased the CSA by an additional 0.5-fold and no further changes in myofiber size were detected after 6 weeks of transgene overexpression (Fig. 5B). We found that the levels of central nucleation were not affected by 2 weeks of transgene activation nor were the number of nuclei per fiber changed at this time point. Interestingly, central nucleation in WT DTG muscle increased to over 20% after 4 and 6 weeks of DOX treatment (Fig. 5C), which correlated with an increase in the number of nuclei per CSA (Fig. 5D). Taken together, this data suggests that Akt1 expression in muscle activates normally quiescent satellite cells, which is further supported by the observation of elevated levels of mRNA transcripts for many satellite cell markers (myoD, pax7, PCNA, myf6 and myogenin) in WT DTG muscle (Table 1; data not shown).

Akt1 increases levels of several compensatory adhesion complexes

To determine the mechanism of rescue for sarcolemma fragility in DTG *mdx* mice, we investigated expression of several adhesion complexes that are known to rescue dystrophin deficiency and restore membrane stability (1–6,16). We found that induction of Akt signaling in *mdx* muscle increased protein expression of the sarcoglycan and dystroglycan subunits to WT levels (Fig. 6). Akt activation increased utrophin protein levels by a minimum of 5- and 10-fold, respectively, in WT and *mdx* DTG muscle, relative to their STG controls
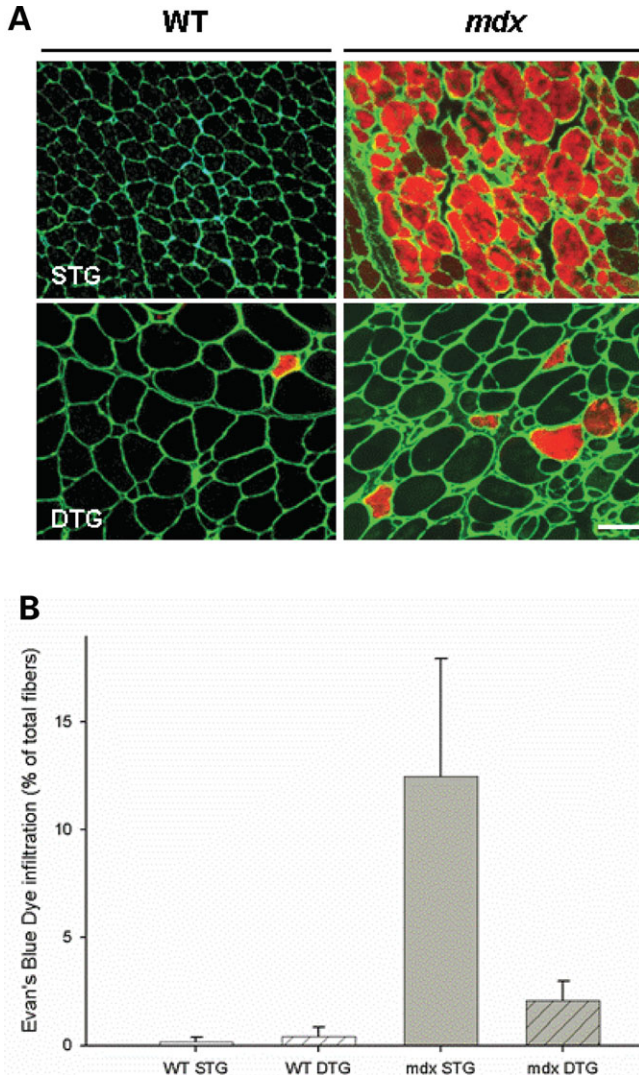
Figure 4. Akt1 activation ameliorates sarcolemmal stability in *mdx* DTG mice. (**A**) Detection of blood serum protein infiltration with Evans Blue dye (EBD) tracer assay. Transverse sections of quadriceps muscle fibers with damaged sarcolemma are shown with red fluorescence. Laminin in the basement membrane is shown with green fluorescence to delineate each myofiber. EBD infiltration was absent in WT STG, detected in low levels in WT DTG and *mdx* DTG mice, and elevated in *mdx* STG mice. Bar, 50 μm. (**B**) Quantification of EBD-positive fibers in whole transverse quadriceps sections. Bars represent percentage of EBD infiltrated fibers in a whole quadriceps section ($\pm$ SEM; Student's *t*-test with Bonferroni adjustment ($\alpha = 0.025$), N.S. WT STG versus WT DTG, *$P < 0.02$, mdx DTG versus *mdx* STG; $n = 3$ mice).

(Fig. 6). Utrophin, an autosomal homologue of dystrophin, replaces dystrophin at the post-synaptic face of the neuromuscular junction to form the UGC (21). In addition to utrophin up-regulation, dystrophin expression is up-regulated by 4-fold in WT DTG muscle thereby increasing overall levels of both DGC and UGC (Fig. 6). Similar to utrophin, integrin α7β1D is up-regulated in a compensatory fashion in *mdx* mice (26) and *Akt* transgene induction increased integrin β1D levels by 3-fold in *mdx* DTG muscle relative to STG controls (Fig. 6). Dysferlin, which mediates membrane repair in a calcium-dependent manner (27), was also increased in both DTG models (Fig. 6).

Immunohistochemical analyses revealed that the UGC and integrin β1D, which are normally restricted to the neuromuscular junction, are broadly localized throughout the extrasynaptic sarcolemma upon Akt expression (Fig. 7). Like utrophin, the skeletal muscle-specific β1D isoform of integrin is enriched at the neuromuscular and myotendinous junctions in WT mice, but has been found to be up-regulated in *mdx* mice (26). Overexpression of α7β1 integrin promotes muscle hypertrophy and regeneration in *mdx/utr$^{-/-}$* mice (28). We found integrin β1 expression homogenously at the sarcolemma in DTG skeletal muscle (Fig. 7).

To further assess the regulation of compensatory complexes, quantitative real-time PCR was performed from skeletal muscle of STG and DTG mice. mRNA levels of several genes including β-DG, α7 integrin, dysferlin and MyoD were significantly elevated in DTG muscle relative to STG controls (Table 1). The observation that mRNA levels of the muscle-specific transcription factor MyoD were tripled in *mdx* DTG muscle supports a role for transcriptional regulation of gene expression upon Akt1 activation. Akt1 regulates skeletal muscle differentiation, at least in part, by enhancing transcriptional activity of MyoD via co-activators p300 and P/CAF (29). In turn, MyoD controls transcription of genes expressed during differentiation including α7 integrin, and several components of the DGC and the UGC (30).

Here we demonstrate that myogenic expression of Akt1 in dystrophin-deficient muscle ameliorates crucial pathologies of muscular dystrophy. Our studies suggest that Akt up-regulates utrophin expression to levels that are sufficient to stabilize the sarcolemma in the absence of dystrophin and thus ameliorate muscular dystrophy. These findings provide a rationale for identification of mechanisms to increase utrophin protein stability or translation as a means to increase utrophin protein expression, in addition to current strategies to identify methods of augmenting utrophin transcription. We demonstrate for the first time that overexpression of a signaling molecule that has been suggested to control hypertrophy (13–17) can diminish the progressive muscle wasting associated with dystrophin deficiency. Akt may represent a critical 'master switch' for myofiber regeneration and modulation of these pathways may have therapeutic value for a broad-range of inherited and acquired muscle wasting disorders.

MATERIALS AND METHODS

Animal models

Mdx female retired breeders were purchased from Jackson Laboratories (Bar Harbor, Maine). DTG mice which were produced by crossing 1256 [3Emut] *MCK-rtTA* transgenic mice expressing the tetracycline transactivator controlled by a mutated skeletal muscle creatine kinase promoter with *TRE-myrAkt1* transgenic mice harboring the constitutively active form of the mouse Akt1 transgene controlled by a tetracycline-responsive promoter. Male DTG mice were bred with *mdx* females to produce four groups of mice used for comparison: (i) Akt STG (either *MCK-rtTA* or *TRE-myrAkt1*) females on an *mdx* heterozygous background, (ii) Akt DTG females on an *mdx* heterozygous background, (iii) Akt STG (either *MCK-rtTA* or *TRE-myrAkt1*) *mdx* males and (iv) Akt
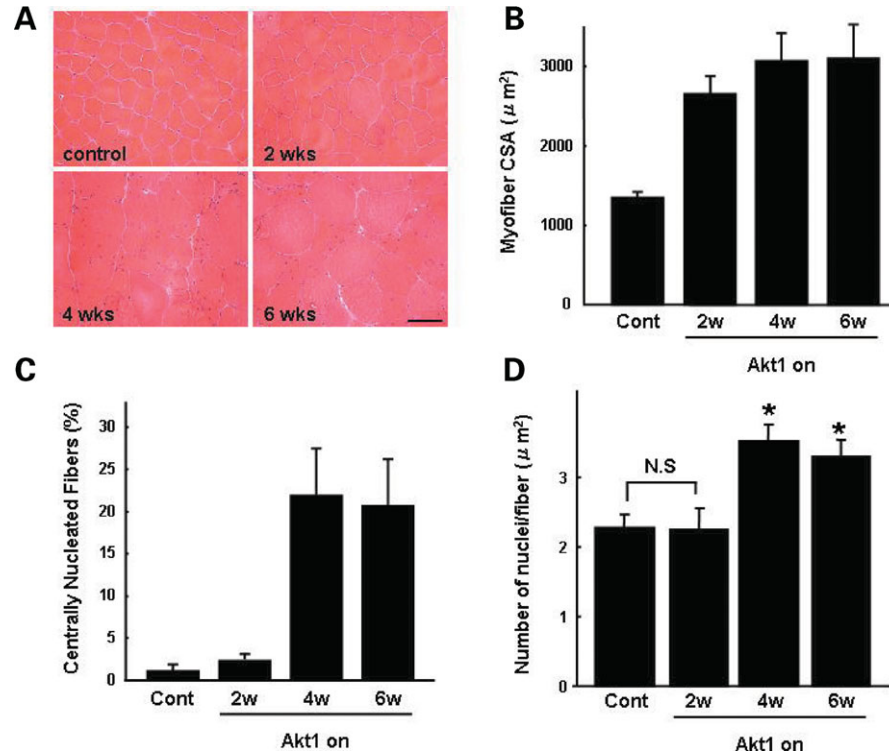
Figure 5. Akt activates muscle regeneration (**A**) Adult WT DTG mice were treated with DOX for two, four and six weeks. Transverse gastrocnemius muscle sections from treated WT DTG mice were stained with hematoxylin and eosin (H&E) to visualize muscle histology. Muscle sections taken from mice treated with vehicle control is shown (control). Note that muscle fiber hypertrophy is evident after two weeks of DOX administration. Bar, 50 μm. (**B**) Cross-sectional area (CSA) of transverse gastrocnemius WT muscle was quantified after two, four and six weeks of DOX treatment. Mean values (μm²) are provided to illustrate overall myofiber hypertrophy that is evident after two weeks of Akt1 transgene activation. Values from control, vehicle-treated muscle are shown. (**C**) Central nucleation (% of total fibers) in gastrocnemius muscle sections was quantified in each group of mice. Regeneration, denoted by the presence of myofibers with centrally placed nuclei, is evident in WT muscle after four weeks of Akt activation. This regeneration is occurring in the absence of muscle pathology or disease. Central nucleation is represented as an average of the % of central nucleation. (**D**) Quantification of the number of nuclei per myofiber is provided. No statistical (N.S.) difference in nuclei per myofiber was observed after two weeks of DOX treatment. After four and six weeks of Akt activation, the number of nuclei/myofiber increased by ∼50% relative to controls. In panels B-D, bars represent standard error of the mean (Fisher's *P* < 0.05; *n* = 7).

Table 1. Akt1-transgene activation mediates changes in mRNA levels

| Gene | Relative mRNA levels | | | |
| | Wild-type | | mdx | |
	STG	DTG	STG	DTG
Utrophin	1.00 ± 0.10	1.09 ± 0.18	0.57 ± 0.22	0.72 ± 0.15
β-DG	1.00 ± 0.16	*1.41 ± 0.17*	*0.61 ± 0.10*	*0.91 ± 0.09*
γ-SG	1.00 ± 0.11	*1.57 ± 0.30*	0.83 ± 0.26	1.01 ± 0.15
ltga-7	*1.00 ± 0.14*	*1.93 ± 0.20*	*0.78 ± 0.07*	*1.81 ± 0.22*
Dysf	*1.00 ± 0.14*	*2.17 ± 0.25*	*0.96 ± 0.11*	*1.86 ± 0.52*
MyoD	*1.00 ± 0.10*	*2.08 ± 0.33*	*0.63 ± 0.11*	*1.87 ± 0.25*

Relative mRNA expression levels of utrophin, β-DG, γ-SG, integrin α7, dysferlin (dysf), MyoD as measured by qRT–PCR. mRNA levels were normalized to internal control gene 36B4 and values are represented relative to WT STG controls. Results are presented as mean ± SEM (*n* = 4). Values in italics are statistically significant in comparisons for STG and DTG control sets (Fisher's, *P* < 0.05).

DTG *mdx* males. To activate Akt transgene expression in DTG mice, three-week-old mice were treated with DOX administered in drinking water (0.5 mg/ml) for a three week period. STG mice (*TRE-myrAkt1* or *MCK-rtTA*) treated with DOX were utilized as controls to eliminate any effect directly related to DOX treatment. After DOX treatment, quadriceps

muscles and total skeletal muscles were harvested, weighed and snap-frozen in liquid nitrogen or mounted in 10.2% polyvinyl alcohol/4.3% polyethylene glycol and rapidly frozen in liquid nitrogen-cooled isopentane. All tissues were stored at −80°C until analyzed. Mice were housed in the Life Sciences Vivarium. All procedures were carried in accordance with guidelines set by the UCLA Institutional Animal Care and Use Committee.

Genotyping of Akt-transgenic *mdx* mice

Akt genotyping. PCR amplifications for transgenes were carried out as previously described (18). Briefly, the *TRE-myrAkt1* transgene was amplified using the following primers: Tet-Akt #1 (5′-CTGGACTACTTGCACTCCGAGA AG-3′) and Tet-Akt #2 (5′-CTGTGTAGGGTCCTTCTTGA GCAG-3′). The cycling conditions were 95°C, 5 min; then 95°C, 30 s and 68°C, 30 s for 30 cycles, followed by 72°C, 10 min. The reaction yielded a 380 bp product. PCR amplifications of the *MCK-rtTA* transgene was amplified using the following primers: MCK-rtTA #1 (5′-CATCTGCGGACTGGA AAAACAAC-3′) and MCK-rtTA #2 (5′-GCATCGGTAAAC ATCTGCTCAAAC-3′). The cycling conditions were 95°C, 5 min; then 94°C, 30 s; 62°C, 30 s and 72°C, 1 min. for 30
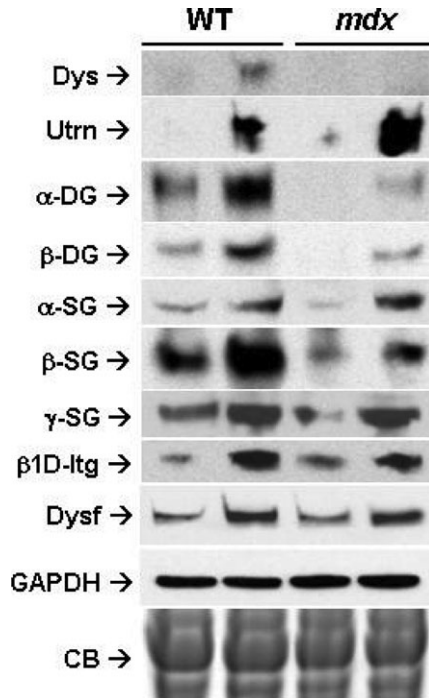
Figure 6. Akt increases expression of compensatory proteins in *mdx* mice. Immunoblotting for several glycoprotein complexes (DGC, UGC, integrin) on skeletal muscle lysates from six-week-old WT STG, WT DTG, *mdx* STG, and *mdx* DTG mice. Identical membranes were probed with antibodies against dystrophin (Dys), utrophin (Utrn), alpha- and beta-dystroglycan (α-DG, β-DG), alpha-, beta- and gamma-sarcoglycan (α-SG, β-SG, γ-SG), β1D integrin and dysferlin (Dysf). GADPH immunoblotting and Coomassie blue (CB) staining of total protein are shown on the bottom panels as a loading controls. Constitutive Akt activation increased the expression of the DGC and UGC in WT mice. Utrophin levels increased in *mdx* mice compared to those of WT mice. Increased expression of β1D integrin and dysferlin was observed upon Akt activation in both WT mice and in *mdx* mice.

cycles, followed by 72°C, 10 min. The reaction yielded a 567 bp product.

Mdx genotyping. The *mdx* point mutation was screened using a modified version of an amplification-resistant mutation system (ARMS) assay (31). Two separate PCR reactions were performed. The WT PCR amplifies the WT dystrophin allele using the following oligonucleotide primers: p260E (5′-GTCACTCAGATAGTTGAAGCCATTTAG-3′) and p306F (5′-CATAGTTATTAATGCATAGATATTCAG-3′). The *mdx* PCR amplifies the *mdx* allele using the following oligonucleotide primers: p259E (5′-GTCACTCAGATAGTT GAAGCCATTTAA-3′) and p306F (5′-CATAGTTATTAAT GCATAGATATTCAG-3′). PCR cycling conditions for both reactions were 95°C, 4 min; then 95°C, 1 min; 55°C, 1 min and 72°C, 1 min for 34 cycles, followed by 72°C, 10 min. Each reaction yielded a 275 bp product. All PCR reactions utilized the GoTaq DNA Polymerase kit (Promega, Madison, WI, USA).

Protein preparation

Snap-frozen skeletal muscles were crushed with liquid nitrogen and a mortar and pestle. Ice-cold RIPA lysis buffer [1%
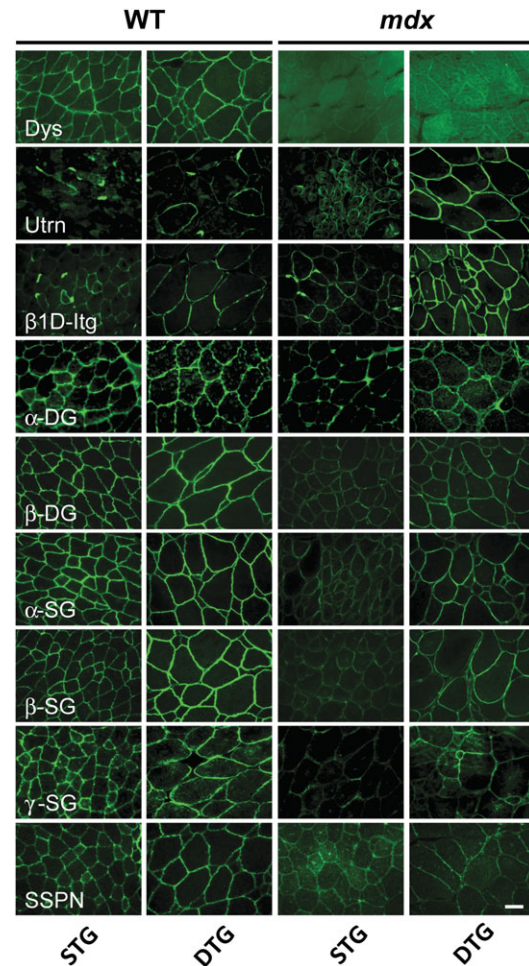

Figure 7. Broad sarcolemmal distribution of compensatory proteins upon Akt activation. Immunohistochemical analyses on transverse quadriceps sections in WT STG, WT DTG, *mdx* STG and *mdx* DTG mice. Sections were stained with antibodies to dystrophin (Dys), utrophin (Utrn), β1D integrin, alpha- and beta-dystroglycan (α-DG, β-DG), alpha-, beta- and gamma-sarcoglycan (α-SG, β-SG, γ-SG) and sarcospan (SSPN), and visualized using indirect immunofluorescence. Increased expression of the DGC and UGC in WT mice was observed upon constitutive activation of Akt1. Akt activation increased expression of only the UGC in *mdx* mice. An increase in utrophin levels was observed in *mdx* mice relative to levels in WT mice. In both WT mice and in *mdx* mice, Akt activation increased the expression of β1D integrin. Bar, 50 μm.

Nonidet P-40, 0.5% sodium deoxycholate, 0.1% sodium dodecyl sulfate (SDS), 1 mM ethylenediaminetetraacetic acid, 5 mM *N*-ethylmaleimide, 50 mM sodium fluoride, 2 mM β-glycerophosphate, 1 mM sodium orthovanadate, 100 nM okadaic acid, 5 nM microcystin LR and 20 mM Tris–HCl, pH 7.6) was utilized for homogenization. Immediately before addition of crushed tissue, protease inhibitors (0.6 μg/ml pepstatin A, 0.5 μg/ml aprotinin, 0.5 μg/ml leupeptin, 0.75 mM benzamidine and 0.1 mM phenylmethylsulfonyl fluoride) were added to the lysis buffer. Homogenates were rocked at 4°C for 1 h. Clarified lysates were obtained following centrifugation at 15 000*g* for 15 min. Clarified tissue lysates were stored at −80°C until analyzed by immunoblot analysis.

Immunoblot analysis

Protein concentrations of clarified tissue lysates were determined using the DC Protein Assay (Bio-Rad). Equal concentrations of protein samples (60 μg) were resolved by 4–20% gradient SDS–PAGE (Pierce, Rockford, IL, USA) and transferred to nitrocellulose membranes (Millipore Corp., Billerica, MA, USA) for subsequent immunoblot experiments. Primary antibodies against Akt, phosphorylated Akt (Ser 473) and phosphorylated GSK3β (Cell Signaling Technologies, Beverly, MA, #9272, #9271 and #9336, respectively) were diluted 1:750. Phosphorylated p70S6K (Cell Signaling Technologies, #9205) was used at a 1:250 dilution. β1D Integrin (Temecula California; International, MAB1900) was diluted 1:100. Primary antibodies against proteins in the DGC and UGC and their respective concentrations include dystrophin (Vector Laboratories, Burlingame, CA, USA; VP-D507, 1:2), utrophin (University of Iowa, Hybridoma Facility; MANCHO3, 1:200), α-DG (Upstate Cell Signaling Solutions, Lake Placid, NY, USA; IIH6, 1:700), β-DG (University of Iowa, Hybridoma Facility; MANDAG2, 1:10), α-SG (Vector Laboratories; VP-A105, 1:20), β-SG (Vector Laboratories; VP-B206, 1:100), γ-SG (Vector Laboratories; VP-G803, 1:200) and SSPN [Rabbit 3 (described previously in 32), 1:50]. α7 Integrin antibody (Santa Cruz Biotechnology, Inc., Santa Cruz, CA; L-17) was diluted 1:100 and α5 integrin (Abcam, Cambridge, UK; ab55988) was diluted 1:50. Anti-dysferlin antibody (Abcam; ab15108) was diluted 1:600. Goat polyclonal antibodies were detected using horseradish peroxidase-conjugated anti-goat IgG (Santa Cruz Biotechnology, Inc.; SC-2033). Rabbit polyclonal antibodies were detected using horseradish peroxidase-conjugated anti-rabbit IgG (Amersham Pharmacia Biotech, Piscataway, NJ, USA, #NA934). Mouse monoclonal primary antibodies were detected by incubating with horseradish peroxidase-conjugated anti-mouse IgG or IgM (Amersham Pharmacia Biotech, 1:3000; Roche Applied Science, Indianapolis, IN, USA; 1:1000, respectively) for 1 h. Immunoblots were developed using enhanced chemiluminescence with SuperSignal West Pico Chemiluminescent Substrate (Pierce, # 34080).

Histology

Hematoxylin and eosin (H&E) staining was used for visualization of fibrosis, central nucleation and cross-sectional fiber area as previously described (11). Transverse quadriceps sections were left at RT for 15 min prior to staining. Briefly, muscle sections were incubated with hematoxylin for 3 min, washed with water for 1 min, incubated with eosin for 3 min, dehydrated in solutions of 70, 80, 90 and 100% ethanol and then incubated in xylene for a total of 10 min. Stained sections were mounted with permount. All supplies for the H&E staining were purchased from Fisher Scientific (Fairlawn, NJ, USA). Centrally nucleated fibers and cross-sectional fiber area were measured from digitized images captured under identical conditions with an Axioplan 2 fluorescent microscope (Carl Zeiss Inc., Thornwood, NY, USA) and Axiovision 4.5 software (Carl Zeiss Inc.). Central nucleation was quantified as a percentage of centrally nucleated fibers over the total number of fibers in an entire transverse quadriceps section. CSA of fiber diameters was calculated using the outline spline function on the Axiovision 4.5 software. For adult studies, DOX treatment was started at the age of 10 weeks.

Evan's blue tracer assay

To assess sarcolemmal permeability, 6-week-old mice were intraperitoneally injected (50 μl per 10 g of body weight) with sterilized EBD (10 mg/ml in sterile 10 mM phosphate buffer, 150 mM NaCl, pH 7.4). Twenty-four hours post-injection, muscles were excised and frozen in liquid nitrogen-cooled isopentane. Transverse quadriceps cryosections (8 μm) were prepared using a CM 3050S cryostat (Leica Microsystems, Bannockburn, IL, USA). Sections were incubated with ice-cold acetone, washed with PBS and blocked for 1 h at RT with 3% BSA diluted in PBS. For sarcolemmal visualization of EBD infiltrated fibers, sections were incubated at 4°C for 18 h with an antibody to laminin (Sigma, St Louis, MO, USA; L 9393) diluted at 1:25 in 1% BSA in PBS. Sections were incubated at RT for 1 h with biotinylated anti-rabbit antibody (Vector Laboratories; BA-1000, 1:250) and then with fluorescein avidin D (Vector Laboratories; A-2001, 1:250). Sections were mounted in VectaShield (Vector Laboratories; H-1000) and imaged using the Axioplan 2 fluorescent microscope with green and blue excitation filters and the Axiovision 4.5 software (Carl Zeiss Inc.). Images were merged using ImageJ software (available on http://rsbweb.nih.gov/ij/). Quantification of sarcolemmal integrity was quantified as a percentage of EBD-positive fibers over the total number of fibers counted in an entire transverse quadriceps section. Data represented is the average percentage of EBD-positive fibers in both quadriceps of each animal.

Immunofluorescence

Transverse sections were prepared from quadriceps muscles as described earlier. All sections, except for those used for detecting α-DG and SSPN, were acclimated to RT for 15 min and then blocked with 3% BSA diluted in PBS for 30 min. The Vector® M.O.M.™ Immunodetection Kit (Vector Laboratories) was then used on these sections following manufacturer's instructions. Primary antibodies diluted in M.O.M. diluent were incubated at 4°C for 18 h against their respective proteins as follows: dystrophin (University of Iowa, Hybridoma Facility; MANDYS1, 1:30), utrophin (Vector Laboratories; VP-U579, 1:5), β1D integrin (Chemicon International; MAB1900, 1:25), β-DG (Vector; VP-B205 1:15), α-SG (Vector Laboratories; VP-A105, 1:30), β-SG (Vector Laboratories; VP-B206, 1:30), γ-SG (Vector Laboratories; VP-G803, 1:15). Afterwards, the sections were incubated with biotinylated anti-mouse antibody (1:250) provided in the M.O.M. kit and then with fluorescein avidin D (Vector Laboratories; A-2001, 1:250). Sections used for detecting α-DG and SSPN were blocked in 3% BSA diluted in PBS followed by primary antibody incubations at 4°C for 18 h as follows: α-DG (Upstate Cell Signaling Solutions; VIA4-1, 1:20) and SSPN (Rabbit 3, 1:5). These primary antibodies were detected by incubating for 1 h with FITC-conjugated anti-mouse secondary antibody or with FITC-conjugated anti-

rabbit secondary antibody (Jackson ImmunoResearch, West Grove, PA; each, 1:500) for α-DG and SSPN, respectively. Sections were mounted in VectaShield (Vector Laboratories). Images were obtained using the Axioplan 2 fluorescent microscope and Axiovision 4.5 software (Carl Zeiss Inc.).

Statistical analyses

Central nucleation, EBD and quadriceps mass data were represented as means $\pm$ SEM. The mean for each variable is calculated as means of the average between the values from the left and right quadriceps of each animal. A two-way ANOVA followed by Fisher's protected least significant difference (Fisher's PLSD) method and the Kruskal–Wallis nonparametric test was used for statistical analysis (Origin 7.0 Software; OriginLab Corporation; Northampton, MA). Values were considered significant when $P < 0.05$. For EBD analysis, the Student's t-test with Bonferroni adjustment to significance at $P < 0.025$ was used. Decreases in EBD fibers in WT DTG relative to WT STG mice could not be observed because levels of EBD-positive fibers were already near zero. Because of this, the two-way ANOVA was not sufficient in assessing the decrease in EBD-positive fibers seen in the *mdx* mice.

Quantitative real-time PCR

Total RNA from whole skeletal muscle was prepared by QIAGEN RNeasy kit using manufacturer protocols. cDNA was produced using the ThermoScript RT–PCR System (Invitrogen). Real-time PCR was performed as described previously (18). Transcript levels were determined relative to the signal from 36B4 and normalized to the mean value of samples from WT STG control mice. Primer sequences for each gene are as follows: utrophin (forward, 5′-GTTTGAG GTGCTTCCTCAGC-3′; reverse, 5′-GCGCTA TCTGGTAG CTGTCC-3′); gene 36B4 (forward, 5′-GCTCC AAGCAGAT GCAGCA-3′; reverse, 5′-CCGGATGTGAGGC AGCAG-3′); β-DG (forward, 5′-CTGGAAGAACCAGCTT GAGG-3′; reverse, 5′-AAATCCGTTGGAATGCTCAC-3′); γ-SG (forward, 5′-TGAAACTGTGGGTTTGACCA-3′; reverse, 5′-GGTACA GCTTCCCATCAGGA-3′); dysferlin (forward, 5′-AACACT GGGTCCCTGTTGAG-3′; reverse, 5′-GCCTCTTCAGTGCT TCCATC-3′); MyoD (forward, 5′-AGCACGCACACTTCCC TACT-3′; reverse, 5′-TCTCGAAG GCCTCATTCACT-3′); integrin α7 (forward, 5′-CTCTGC GTTCCTCAACATCA-3′; reverse, 5′-TGTGCTAGGCTCCA CCTTCT-3′).

SUPPLEMENTARY MATERIAL

Supplementary Material is available at *HMG* online.

ACKNOWLEDGEMENTS

We thank Dr M. Song and J.L. Marshall (UCLA) for technical assistance.

Conflict of Interest statement. None declared.

REFERENCES

1. Hoffman, E.P., Brown, R.H. and Kunkel, L.M. (1987) Dystrophin: the protein product of the Duchenne muscular dystrophy locus. *Cell*, **51**, 919–928.
2. Ohlendieck, K. and Campbell, K.P. (1991) Dystrophin: the protein product of the Duchenne muscular dystrophy locus. *J. Cell Biol.*, **115**, 1685–1694.
3. Ervasti, J.M., Ohlendieck, K., Kahl, S.D., Gaver, M.G. and Campbell, K.P. (1990) Deficiency of a glycoprotein component of the dystrophin complex in dystrophic muscle. *Nature*, **345**, 315–319.
4. Durbeej, M. and Campbell, K.P. (2002) Muscular dystrophies involving the dystrophin-glycoprotein complex: an overview of current mouse models. *Curr. Opin. Genet. Dev.*, **12**, 349–361.
5. Heydemann, A. and McNally, E.M. (2007) Consequences of disrupting the dystrophin-sarcoglycan complex in cardiac and skeletal myopathy. *Trends Cardiovasc. Med.*, **17**, 55–59.
6. Campbell, K.P. and Kahl, S.D. (1989) Association of dystrophin and an integral membrane glycoprotein. *Nature*, **338**, 259–262.
7. Ervasti, J.M. and Campbell, K.P. (1991) Membrane organization of the dystrophin-glycoprotein complex. *Cell*, **66**, 1121–1131.
8. Ervasti, J.M., Kahl, S.D. and Campbell, K.P. (1991) Purification of dystrophin from skeletal muscle. *J. Biol. Chem.*, **266**, 9161–9165.
9. Ervasti, J.M. and Campbell, K.P. (1993) A role for the dystrophin–glycoprotein complex as a transmembrane linker between laminin and actin. *J. Cell Biol.*, **122**, 809–823.
10. Yoshida, M. and Ozawa, E. (1990) Glycoprotein complex anchoring dystrophin to sarcolemma. *J. Biochem.*, **108**, 748–752.
11. Peter, A.K. and Crosbie, R.H. (2006) Hypertrophic response of Duchenne and limb-girdle muscular dystrophies is associated with activation of Akt pathway. *Exp. Cell Res.*, **312**, 2580–2591.
12. Dogra, C., Changotra, H., Wergedal, J.E. and Kumar, A. (2006) Regulation of phosphatidylinositol 3-kinase (PI3K)/Akt and nuclear factor-kappa B signaling pathways in dystrophin-deficient skeletal muscle in response to mechanical stretch. *J. Cell Physiol.*, **208**, 575–585.
13. Rommel, C., Bodine, S.C., Clarke, B.A., Rossman, R., Nunez, L., Stitt, T.N., Yancopoulos, G.D. and Glass, D.J. (2001) Mediation of IGF-1-induced skeletal myotube hypertrophy by PI(3)K/Akt/mTOR and PI(3)K/Akt/GSK3 pathways. *Nat. Cell Biol.*, **3**, 1009–1013.
14. Takahashi, A., Kureishi, Y., Yang, J., Luo, Z., Guo, K., Mukhopadhyay, D., Ivashchenko, Y., Branellec, D. and Walsh, K. (2002) Myogenic Akt signaling regulates blood vessel recruitment during myofiber growth. *Mol. Cell Biol.*, **22**, 4803–4814.
15. Bodine, S.C., Stitt, T.N., Gonzalez, M., Kline, W.O., Stover, G.L., Bauerlein, R., Zlotchenko, E., Scrimgeour, A., Lawrence, J.C., Glass, D.J. and Yancopoulos, G.D. (2001) Akt/mTOR pathway is a crucial regulator of skeletal muscle hypertrophy and can prevent muscle atrophy *in vivo*. *Nat. Cell Biol.*, **3**, 1014–1019.
16. Barton, E.R., Morris, L., Musaro, A., Rosenthal, N. and Sweeney, H.L. (2002) Muscle-specific expression of insulin-like growth factor I counters muscle decline in mdx mice. *J. Cell Biol.*, **157**, 137–148.
17. Pallafacchina, G., Calabria, E., Serrano, A.L., Kalhovde, J.M. and Schiaffino, S. (2002) A protein kinase B-dependent and rapamycin-sensitive pathway controls skeletal muscle growth but not fiber type specification. *Proc. Natl. Acad. Sci. USA*, **99**, 9213–9218.

18. Izumiya, Y., Hopkins, T., Morris, C., Sato, K., Zeng, L., Viereck, J., Hamilton, J.A., Ouchi, N., LeBrasseur, N.K. and Walsh, K. (2008) Fast/ Glycolytic muscle fiber growth reduces fat mass and improves metabolic parameters in obese mice. *Cell Metab.*, **7**, 159–172.

19. Kandarian, S.C. and Jackman, R.W. (2006) Intracellular signaling during skeletal muscle atrophy. *Muscle Nerve*, **33**, 155–165.

20. Neri, L.M., Borgatti, P., Capitani, S. and Martelli, A.M. (2002) The nuclear phosphoinositide 3-kinase/AKT pathway: a new second messenger system. *Biochim. Biophys. Acta*, **1584**, 73–80.

21. Tinsley, J., Deconinck, N., Risher, R., Kahn, D., Phelps, S., Gillis, J.M. and Davies, K. (1998) Expression of full-length utrophin prevents muscular dystrophy in *mdx* mice. *Nat. Med.*, **4**, 1441–1444.

22. Tinsley, J.M., Potter, A.C., Phelps, S.R., Fisher, R., Trickett, J.I. and Davies, K.E. (1996) Amelioration of the dystrophic phenotype of *mdx* mice using a truncated utrophin transgene. *Nature*, **384**, 349–353.

23. McArdle, A., Edwards, R.H. and Jackson, M.J. (1994) Time course of changes in plasma membrane permeability in the dystrophin-deficient mdx mouse. *Muscle Nerve*, **17**, 1378–1384.

24. Rosenberg, M.I., Georges, S.A., Asawachaicharn, A., Analau, E. and Tapscott, S.J. (2006) MyoD inhibits Fstl1 and Utrn expression by inducing transcription of miR-206. *J. Cell Biol.*, **175**, 77–85.

25. Cassano, M., Biressi, S., Finan, A., Benedetti, L., Omes, C., Boratto, R., Martin, F., Allegretti, M., Broccoli, V., Cusella De Angelis, G. *et al.* (2008) Magic-factor 1, a partial agonist of Met, induces muscle hypertrophy by protecting myogenic progenitors from apoptosis. *PLoS ONE*, **3**, e3223.

26. Hodges, B.L., Hayashi, Y.K., Nonaka, I., Wang, W., Arahata, K. and Kaufman, S.J. (1997) Altered expression of the alpha7beta1 integrin in human and murine muscular dystrophies. *J. Cell Sci.*, **110**, 2873–2881.

27. Bansal, D., Miyake, K., Vogel, S.S., Groh, S., Chen, C.C., Williamson, R., McNeil, P.L. and Campbell, K.P. (2003) Defective membrane repair in dysferlin-deficient muscular dystrophy. *Nature*, **423**, 168–172.

28. Burkin, D.J., Wallace, G.Q., Milner, D.J., Chaney, E.J., Mulligan, J.A. and Kaufman, S.J. (2005) Transgenic expression of {alpha}7{beta}1 integrin maintains muscle integrity, increases regenerative capacity, promotes hypertrophy, and reduces cardiomyopathy in dystrophic mice. *Am. J. Pathol.*, **166**, 253–263.

29. Wilson, E.M. and Rotwein, P. (2007) Selective control of skeletal muscle differentiation by Akt1. *J. Biol. Chem.*, **282**, 5106–5110.

30. Tapscott, S.J. (2005) The circuitry of a master switch: Myod and the regulation of skeletal muscle gene transcription. *Development*, **132**, 2685–2695.

31. Rooney, J.E., Welser, J.V., Dechert, M.A., Flintoff-Dye, N.L., Kaufman, S.J. and Burkin, D.J. (2006) Severe muscular dystrophy in mice that lack dystrophin and alpha7 integrin. *J. Cell Sci.*, **119**, 2185–2195.

32. Miller, G., Peter, A.K., Espinoza, E., Heighway, J. and Crosbie, R.H. (2006) Over-expression of Microspan, a novel component of the sarcoplasmic reticulum, causes severe muscle pathology with triad abnormalities. *J. Muscle Res. Cell Motil.*, **27**, 545–558.